

Compression of Medical images using SPIHT Algorithm for Telemedicine Application

Jins Sebastian¹, Deny J² and Kumar S. N³

¹Research Scholar, Kalasalingam Academy of Research and Education, Krishnankoil, Tamilnadu, India, jinsarackaparampil@amaljyothi.ac.in

²Department of Electronics and Communication Engineering, Kalasalingam Academy of Research and Education, Krishnankoil, Tamilnadu, India; j.deny@klu.ac.in

³Department of Electrical and Electronic Engineering, Amal Jyothi College of Engineering, Kanjirappally, Kerala, India; appu123kumar@gmail.com

*Correspondence: J. Deny; E-mail: j.deny@klu.ac.in

ABSTRACT- Image compression plays a pivotal role in the medical field for the storage and transfer of DICOM images. This research work focuses on the compression of medical images using Set Partitioning in Hierarchy Trees (SPIHT) algorithm. The CT/MR images are used as input, the images are subjected to filtering by a median filter. The CT images in general are corrupted by Gaussian noise and MR images are corrupted by rician noise. The SPIHT algorithm comprises of following phases; transformation into wavelet domain, refinement pass and sorting pass. The Haar wavelet transform is employed and the wavelet coefficients are subjected to sorting and refinement pass. The Haar wavelet transform generates LL, HL, HL and HH sub-bands. In the sorting pass, the coefficients are classified into significant and insignificant. The refinement pass creates the precision bits for the significant coefficients. The main characteristic of the SPIHT algorithm is that it does not use an entropy coder. The reconstructed image in the decoding stage was validated by performance metrics. The SPIHT algorithm generates proficient results, when compared with the classical algorithms like wavelet and embedded zero tree wavelet (EZW) algorithms.

Keywords: Wavelet, EZW, SPIHT, Compression, COVID 19.

ARTICLE INFORMATION

Author(s): Jins Sebastian, J. Deny and S.N. Kumar;

Received: 28/10/23; **Accepted:** 15/01/24; **Published:** 05/02/24;

E- ISSN: 2347-470X;

Paper Id: IJEER231020;

Citation: 10.37391/IJEER.120108

Webpage-link:

<https://ijeer.forexjournal.co.in/archive/volume-12/ijeer-120108.html>



Publisher's Note: FOREX Publication stays neutral with regard to jurisdictional claims in Published maps and institutional affiliations.

1. INTRODUCTION

Image processing role is inevitable in the medical domain for disease diagnosis and surgical preplanning. The image compression objective is to minimize the file size, thereby aiding proficient storage and data transmission. The multiscale transforms are employed in [1] for the compression of CT, MR and mammogram images. The fast Fourier transform with game optimization was employed in [2] for the compression of ultrasound and MR images, proficient results are produced, when compared with the classical compression techniques. The prediction technique was incorporated in wavelet transform for the compression of MR and ultrasound images [3]. The wavelet and curvelet transform were utilized in [4] for the compression of CT images, the contourlet transform was found to be proficient with better edge preservation. The DCT with adaptive thresholding was utilized in [5] for the compression of X-ray, CT and Ultrasound images. The genetic algorithm along with

the DCT algorithm was deployed in [6] for the compression of MR images.

The bitplane technique was deployed with DWT in [7] for the compression and it relies on ROI. The multiple array technique was used in [8] for the compression of medical images, lossy and lossless algorithms are discussed, the multiple array technique was found to be efficient for telemedicine applications. A fair analysis of JPEG and JPEG 2000 was projected in [9] for compression, the JPEG 2000 results are robust when related to the JPEG algorithm. The embedded zero tree wavelet algorithm was put forward in [10] for the compression of medical images and the results were found to be efficient when compared with the JPEG algorithm. A distinction of wavelet transforms, Quincunx wavelet coupled with SPIHT for the compression of the 3D data set, the results were robust, when compared with the classical approaches [11]. The compressed CT images of the chest by JPEG algorithm were utilized in the classification of COVID-19 using deep learning algorithm [12].

The lossless compression of medical images for region-based coding (RBC) using DWT and SPIHT algorithm to enhance the quality of ROI in compression was proposed in [13]. The SPIHT compression model was incorporated with various transforms and assessed their performance [14]. The 3D SPIHT algorithm at different bits per pixel was used along with DWT and DTCWT for the compression of 4D Medical Images [15]. A lossless compression ROI-based algorithm based on Vector Quantization and SPIHT was proposed for the compression of 2D and 3D medical images [16]. A hybrid algorithm

compression algorithm was proposed with SVD and SPIHT for the compression of medical images [17]. The SPIHT algorithm is used for the compression of Stego images in the medical data framework for telehealth applications. [18]. The hybrid integer wavelet transforms (IWT), lossless Hadamard transform (LHT) and Arithmetic compression algorithm provides good compression of medical images [19]. A high compression ratio is achieved by Coefficient Mixed Thresholding based Adaptive Block Compressed Sensing (CMT-ABCS) in the medical images which reconstruct with only 10% of samples [20]. An ROI-based compression algorithm was implemented in the medical image using DCT with Huffman Run-length encoding for ROI and Capsule Autoencoder for non-ROI regions. [21]. Shape adaptive discrete wavelet transform 3D-BISK algorithm was used for the ROI-based compression of 3D MRI Brain Datasets for Wireless transmission [22]. The compression algorithms are highlighted in section 2, results and discussion are put forward in section3, the conclusion is drawn in section 3.

2. MATERIALS AND METHODS

This research work performs the comparative analysis of transform domain approaches for the compression of medical images. The SPIHT algorithm generates proficient results when compared with the Wavelet and EZW algorithms. Figure 1 depicts the overall flow diagram of the compression model utilized in this research work.

2.1 Data Acquisition

The COVID-19 CT images were obtained from the public database <https://data.mendeley.com/datasets/8h65ywd2jr/3> [23]. The abdomen CT and MR brain images were obtained from Metro scans and the Research laboratory, Trivandrum.

2.2 Medical Image Compression using SPIHT Algorithm

The set partitioning in the hierarchical tree approach is developed and used for lossless image compression, which is an improvement of the EZW technique. SPIHT is a wavelet-based image compression method and is one of the most powerful compression techniques. The major benefits of the SPIHT technique are that it provides, good image quality while maintaining a high PSNR. It is the most effective way for the transmission of progressive images. The SPIHT algorithm achieves excellent compression results, when compared with the classical compression models. The first phase in the SPIHT algorithm is the decomposition of the input image into wavelet coefficients and the spatial orientation tree is formulated. The decomposed coefficients are subjected to encoding process from MSB planes to LSB planes, started with highest coefficient value. There are two stages in the SPIHT algorithm; sorting and refining stage. The sorting stage checks for zero trees and arrange the insignificant coefficients based on the threshold value. The refining stage is a one-scan pass and it is terminated, when the desired bit rate is reached. The SPIHT algorithm yields proficient results without an entropy coder in terms of computational complexity. Furthermore, in the sorting pass, it employs a subset partitioning technique to limit the number of magnitude comparisons, lowering the algorithm's

computational cost. Finally, SPIHT's progressive mode allows the coding/decoding process to be interrupted at any point throughout the compression process. Despite these benefits, SPIHT has drawbacks such as huge memory requirements and delays.

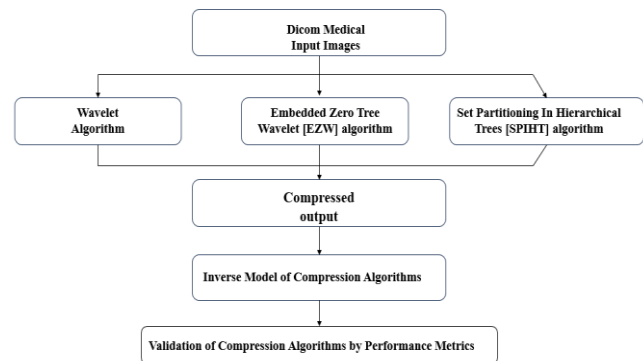


Figure 1: Overall flow diagram of the compression model

2.2.1. SPIHT Algorithm Steps

1. **Initialization:** Define the number of decomposition stages first during the initialization stage. The threshold value is preset and the list of significant and insignificant pixels is created, and those with offspring to the insignificant sets list as type A entries.
2. **Sorting Pass:** The sorting stage comprises two steps as follows
 - i. *Generation of List of Insignificant Pixels:* The first step in the sorting process is the detection of insignificant pixels and it is collected. The collected pixel list is scanned to check, whether it is significant. An output bit of 1 is created when the pixel is significant and for sign representation, again 0 or 1 is used, when the coefficient value is positive or negative. When the input is insignificant, it is marked as 0, followed by a bit for the coefficient's sign.
 - ii. *Generation of List of Insignificant Sets:* Examining the entries in LIS is the second stage of the sorting pass. To begin, determine if the entry is kind A or type B. When an entry is the set of all descendants of a type A coefficient, the magnitude tests are applied to all offspring of the present entry to determine whether they are significant. If the entry is determined to be significant, the entry's immediate offspring are subjected to magnitude tests. If there is a substantial number of direct offspring, it is transferred to LSP; otherwise, it is moved to LIP, as in the previous stage.
 - iii. The insignificant pixels entry is pushed to the end of LIS as type B, which is the set of all descendants of a coefficient save the immediate offspring (children). If the LIS entry is type B, the descendants of its immediate offspring are subjected to a significance test. If the significance test is true, the spatial orientation tree with the root of type B entry is divided into four sub-trees, each of which is rooted by the direct offspring, and these direct children are appended to the end of the LIS as type A entries, while the type B entry is removed.

- Refinement pass:** At the current threshold, it is utilized to output the refined bits of the coefficients in LSP. The current threshold, $T/2$, is halved before the algorithm moves on to the next phase.
- Quantization-Step Update:** Go to step 2 after decreasing n by one. This procedure continues until the final quantization level equals 1.

3. RESULTS AND DISCUSSION

This research work utilizes wavelet, EZW and SPIHT compression algorithm developed in MATLAB 2022a for the compression of medical images. The comparative analysis of SPIHT algorithm results with Wavelet and EZW algorithms are done with the aid of metrics.

Let $I(i, j)$ and $R(i, j)$ represents the input image and reconstructed image pixel values, the performance metrics. *Figure 2* depicts the SPIHT algorithm reconstructed outputs corresponding to the abdomen CT data set (ID1-ID4). *Table 1* and 2 represents the performance metrics corresponding to the data set (ID1-ID4). *Figure 3* depicts the SPIHT algorithm reconstructed outputs corresponding to the COVID 19 CT data set (ID5-ID8). *Table 3 and 4* represents the performance metrics corresponding to the data set (ID5-ID8). *Figure 4* depicts the SPIHT algorithm reconstructed outputs corresponding to the COVID 19 CT data set (ID9-ID12). *Table 5 and 6* represents the performance metrics corresponding to the data set (ID9-ID12).

The expression for Peak signal to noise ratio (PSNR) is as follows; The larger value of PSNR greater than 25db is an efficient indication of reconstructed image quality

$$PSNR = 10 \log \left(\frac{255^2}{MSE} \right) \quad (1)$$

The expression for the compression Ratio is as follows

$$CR = \frac{\text{Size of the uncompressed image}}{\text{Size of the compressed image}} \quad (2)$$

The expression for Normalized Cross Correlation (NCC) is as follows

$$NCC = \frac{\sum_{i=1}^m \sum_{j=1}^n \frac{I(i,j)*R(i,j)}{I(i,j)^2}}{\sum_{i=1}^m \sum_{j=1}^n I(i,j)^2} \quad (3)$$

The expression for Normalized Absolute Error (NAE) is as follows

$$NAE = \frac{\sum_{i=1}^m \sum_{j=1}^n (I(i,j)-R(i,j))}{\sum_{i=1}^m \sum_{j=1}^n I(i,j)} \quad (4)$$

The expression for Average Difference (AD) is as follows

$$AD = \frac{1}{mn} \sum_{i=1}^m \sum_{j=1}^n [I(i, j) - R(i, j)] \quad (5)$$

The expression for Structural Content (SC) is as follows

$$SC = \frac{\sum_{I=1}^M \sum_{J=1}^N (I(i,j))^2}{\sum_{I=1}^M \sum_{J=1}^N (R(i,j))^2} \quad (6)$$

The expression for Laplacian Mean square error (LMSE) is as follows

$$LMSE = \frac{\sum_{I=1}^m \sum_{J=1}^n [L(I(i,j)) - L(R(i,j))]^2}{\sum_{I=1}^m \sum_{J=1}^n [L(I(i,j))]^2} \quad (7)$$

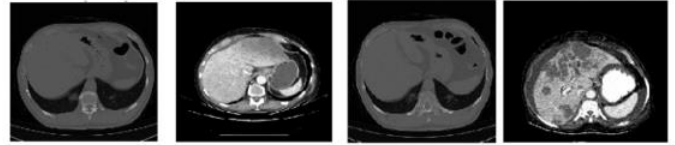


Figure 2: SPIHT reconstructed output corresponding to the abdomen CT data set (ID1 – ID4)

Table 1. Performance metrics of SPIHT Transform Based Image Compression for abdomen CT DICOM Images

Image ID	PSNR	AD	SC	NK	MD	LMSE	NAE
ID1	38.98	0.007	1.0013	0.9983	13.59	0.27	0.048
ID2	38.24	-0.012	0.999	0.9997	27.25	0.096	0.03
ID3	38.50	-0.0033	1.0011	0.9983	14.875	0.2847	0.0485
ID4	36.256	-0.010	1.0001	0.9991	30.163	0.134	0.0418

Table 2. Execution time of SPIHT algorithm in seconds for abdomen CT Images

Images	ID1	ID2	ID3	ID4
Time (seconds)	25.74	19.60	27.24	18.935

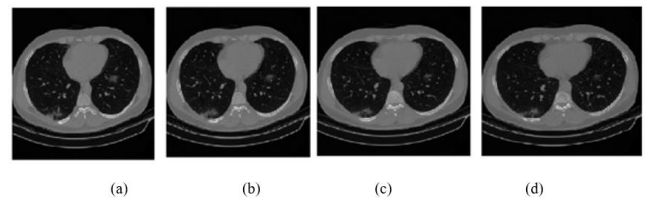


Figure 3: SPIHT reconstructed output corresponding to the COVID 19 CT data set (ID5 – ID8)

Table 3. Performance metrics of SPIHT Transform Based Image Compression for COVID-19 CT DICOM Images

Images ID	PSNR	AD	SC	NK	MD	LMSE	NAE
ID5	43.35	0.0014	1.00	0.99	9.29	0.26	0.03
ID6	43.40	-0.0014	1.00	0.99	7.79	0.26	0.030
ID7	43.41	-0.0007	1.00	0.99	9.26	0.26	0.03
ID8	43.64	-0.0021	1.00	0.99	8.19	0.26	0.031

Table 4. Execution time of SPIHT algorithm in seconds for COVID-19 CT Images

Images	ID5	ID6	ID7	ID8
Time (seconds)	23.33	57.16	38.90	71.51

Table 5. Performance metrics of SPIHT Transform Based Image Compression for MR brain DICOM Images

Images ID	PSNR	AD	SC	NK	MD	LMSE	NAE	Time
ID9	40.90	0.009	1.00	0.99	14.37	0.18	0.05	2.53
ID10	40.73	0.002	1.00	0.99	30.64	0.19	0.05	2.03
ID11	39.39	0.003	1.01	0.99	14.44	0.20	0.06	1.90
ID12	39.18	0.010	1.01	0.99	15.75	0.20	0.06	1.90

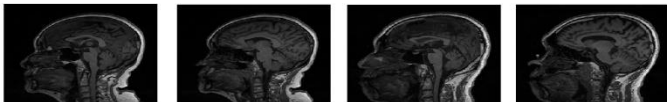


Figure 4: SPIHT reconstructed output corresponding to the MR brain data set (ID9 – ID12)

Table 6. Execution time of SPIHT algorithm in seconds for MR brain DICOM Images

Images	ID9	ID10	ID11	ID12
Time (seconds)	2.53	2.03	1.90	1.90

The inferences for the results corresponding to the tables 1 and 2 are as follows

- $36 < PSNR < 39$: (> 25dB is good)
- $-0.0033 < AD < 0.007$: Low value is good
- SC: Almost equal to 1
- $0.9983 < NK < 0.9997$: Nearby 1 is good
- $13 < MD < 31$: Low value is good
- $0.096 < LMSE < 0.3$: Low value is good
- $0.03 < NAE < 0.049$: Low value is good
- $18 \text{ seconds} < \text{Time} < 28 \text{ seconds}$: Low value is good
- CR=8: (High value favours low storage space and low value favours high storage space)

The inferences for the results corresponding to the tables 3 and 4 are as follows

- $43.3 < PSNR < 43.6$: (> 25dB is good)
- $-0.002 < AD < .0014$: Low value is good
- SC: Almost equal to 1
- NK=.99: Nearby 1 is good
- $7.79 < MD < 9.29$: Low value is good
- LMSE=.26: Low value is good
- $0.03 < NAE < 0.031$: Low value is good
- $23.3 \text{ seconds} < \text{Time} < 71.5 \text{ seconds}$: Low value is good
- CR=8: (High value favours low storage space and low value favours high storage space)

The inferences for the results corresponding to the tables 5 and 6 are as follows

- $39 < PSNR < 41$: (> 25dB is good)
- $-0.002 < AD < 0.01$: Low value is good
- SC: Almost equal to 1
- NK=.99: Nearby 1 is good
- $14.3 < MD < 30.7$: Low value is good
- $0.18 < LMSE < 0.20$: Low value is good
- $0.05 < NAE < 0.06$: Low value is good
- $1.9 \text{ seconds} < \text{Time} < 2.6 \text{ seconds}$: Low value is good

- CR=8: (High value favours low storage space and low value favours high storage space)

The mean values of performance metrics for the data sets are represented in figures 5-12. The performance metrics plots reveal the efficiency of the SPIHT algorithm in the compression of medical images, when compared with the wavelet and EZW algorithms.

Wavelet-based methods efficiently handle different frequency components in data, supporting both high and low resolutions. Wavelet compression allows gradual data transmission, providing a broad overview initially that can be refined progressively. Implementing wavelet transforms can be computationally demanding, particularly for larger datasets or real-time applications. Wavelet transforms might introduce artifacts along boundaries, impacting the accuracy of reconstructed data.

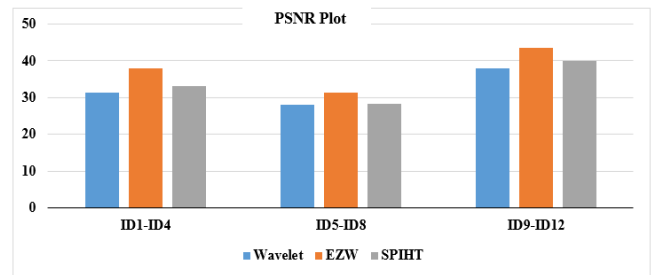


Figure 5: PSNR plot of compression algorithms

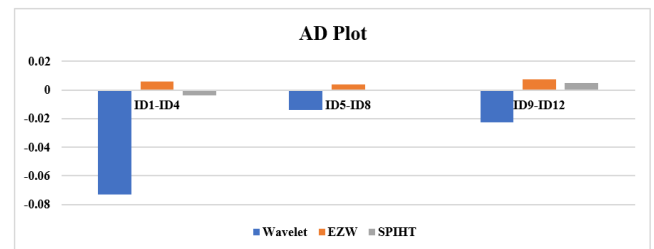


Figure 6: AD plot of compression algorithms

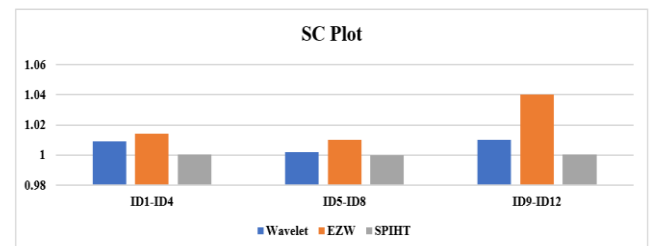


Figure 7: SC plot of compression algorithms

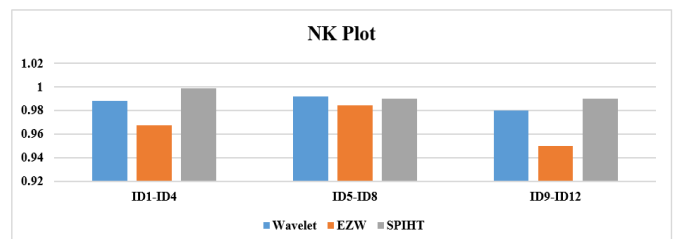


Figure 8: NK plot of compression algorithms

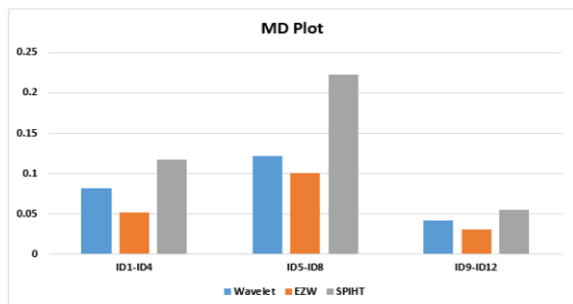


Figure 9: MD plot of compression algorithms

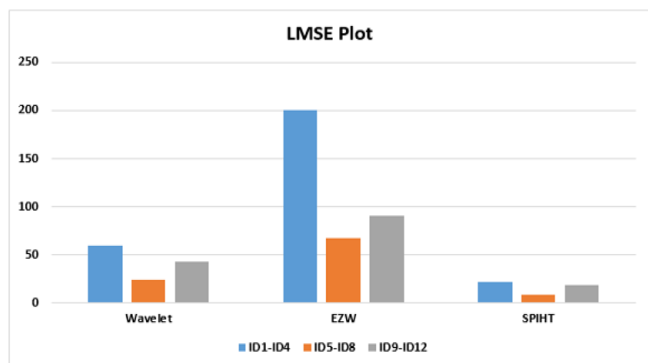


Figure 10: LMSE plot of compression algorithms

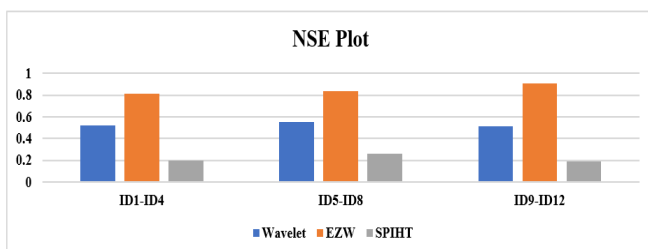


Figure 11: NSE plot of compression algorithms

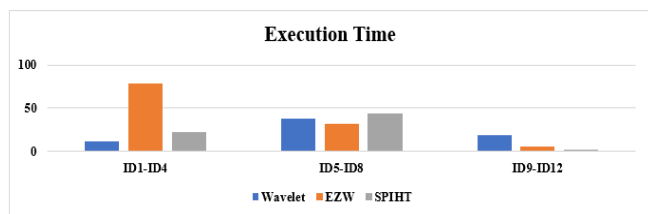


Figure 12: Execution time plot of compression algorithms

EZW offers gradual decoding and transmission, allowing for adding detailed information to encoded data in stages. EZW achieves high compression by efficiently representing data with fewer bits. The encoding process in EZW demands high computation, making it less suitable for real-time applications or devices with limited processing power. SPIHT supports progressive transmission, efficiently streaming data with increasing detail levels. SPIHT efficiently uses spatial redundancies in images for high compression while maintaining quality. Like other wavelet-based methods, SPIHT's implementation complexity and computational load can be high. In terms of the reconstructed image quality, the performance of the SPIHT algorithm was found to be superior, when compared with the wavelet and EZW algorithms. The

comparison of the proposed algorithms with some of the related works is depicted in Table 7.

Table 7. Comparison of the proposed algorithm with the related works

Algorithm Details	Inferences
Difference Transform [24]	Difference Transform algorithms offer potential alternatives to traditional transforms like the Cosine or Wavelet. When compared to established medical image standards like TIFF or PNG, they can often compete favorably and, in many scenarios, exhibit superior performance
ROI-based compression comprising of SPIHT coupled with vector quantization [25]	Tested on MR brain images; PSNR>35 dB, the average compression ratio is 20%, low bits per pixel values
Singular Value Decomposition (SVD) and SPIHT algorithm [26]	Tested on MRI and X-ray images; PSNR>40 dB, hybrid compression model generates proficient results, when compared with the SPIHT and the SVD algorithms
Proposed compression model (SPIHT)	Tested on CT and MR images; PSNR>32 dB, SC>0.9, NK>0.9

In telemedicine, where networks often have limited capacity, compression models shrink the size of medical data. This efficient sizing enables smoother data transfer, especially in remote or resource-constrained areas. By reducing file sizes, compression models speed up the transfer of medical data. This quick transmission is vital for real-time consultations, emergencies, or remote diagnostics where prompt access to information impacts patient care. Efficient compression cuts down data storage and transmission expenses for telemedicine services. This is particularly beneficial for healthcare systems handling large data volumes, helping manage costs linked to data storage and network use. Compression allows easier sharing of medical information across different devices and platforms. This accessibility fosters collaboration among healthcare professionals located in various places. Compression, especially lossless methods, maintains the integrity of medical images, reports, or records. This ensures essential details remain intact, crucial for accurate diagnosis and treatment. Efficient compression models address technical challenges, making data transmission and storage smoother. This ease encourages healthcare providers to embrace telemedicine more readily. Compression models for telemedicine often integrate security measures, ensuring compliance with privacy regulations. This is crucial for maintaining patient confidentiality and preventing unauthorized access to health information.

4. CONCLUSION

This research work proposes a comparative analysis of transform domain approaches for the compression of medical DICOM images. The SPIHT algorithm results were found to be proficient when compared with the wavelet and the EZW approaches. The SPIHT algorithm showed better performance as compared to the existing algorithms. The compressions were done using real-time medical images, SPIHT algorithm aims to achieve a high compression ratio along with good image quality. The performance metrics were used for the evaluation

and the average values were also determined. The high compression ratio makes the management of medical images more effective because of the reduced storage requirements.

5. ACKNOWLEDGMENTS

The author would like to express his heartfelt gratitude to the supervisor for his guidance and unwavering support during this research for his guidance and support.

REFERENCES

- [1] Raja, S.P. (2019). Joint medical image compression-encryption in the cloud using multiscale transform-based image compression encoding techniques. *Sādhanā*, 44(2), 28.
- [2] Li, L., Muneeswaran, V., Ramkumar, S., Emayavaramban, G., Gonzalez, G.R. (2019). Metaheuristic FIR filter with game theory-based compression technique-A reliable medical image compression technique for online applications. *Pattern Recognition Letters*, 125, 7-12.
- [3] Eben Sophia, P., Anitha, J. (2017). Contextual medical image compression using normalized wavelet-transform coefficients and prediction. *IETE Journal of Research*, 63(5), 671-83.
- [4] Riazifar, N., Yazdi, M. (2009). Effectiveness of contourlet vs wavelet transform on medical image compression: a comparative study. *World Academy of Science, Engineering and Technology*, 49(3), 837- 42.
- [5] Singh, S., Kumar, V., Verma, HK. (2007). Adaptive threshold-based block classification in medical image compression for teleradiology. *Computers in Biology and Medicine*, 37(6), 811-9.
- [6] Shih, FY., Wu, Y.T. (2005). Robust watermarking and compression for medical images based on genetic algorithms. *Information Sciences*, 175(3), 200-16.
- [7] Lee, HK., Kim, H.J., Kwon, KR., Lee, J.K. (2005). ROI medical image watermarking using DWT and bit-plane. In 2005 Asia-Pacific Conference on Communications, 512-515.
- [8] Devaraj, K., Munukur, R.K., Kesavamurthy, T. (2005). Lossless medical-image compression using multiple array technique. In 2005 International Symposium on Intelligent Signal Processing and Communication Systems, pp. 837-840.
- [9] OH, TH., Besar, R. (2002). Medical image compression using JPEG-2000 and JPEG: A comparison study. *Journal of Mechanics in Medicine and Biology*, 2 (03n04), 313-28.
- [10] Dilmaghani, R.S., Ahmadian, A., Ghavami, M., Aghvami, A.H. (2004). Progressive medical image transmission and compression. *IEEE signal processing letters*, 11(10), 806-9.
- [11] Haouari, B. (2020). 3D Medical image compression using the quincunx wavelet coupled with SPIHT. *Indonesian J. Electric Eng. Comput. Sci.*, 18, 821
- [12] Zhu, Z., Xingming, Z., Tao, G., Dan, T., Li, J., Chen, X., Li, Y., Zhou, Z., Zhang, X., Zhou, J., Chen, D. (2021). Classification of COVID-19 by compressed chest CT image through deep learning on a large patient's cohort. *Interdisciplinary Sciences: Computational Life Sciences*, 13(1), 73-82.
- [13] Mukhopadhyay, A.P., Mohapatra, S., Bhattacharya, B. (2019). Roi based medical image compression using dwt and spiht algorithm. In 2019 international conference on vision towards emerging trends in communication and networking (ViTECoN), 1-5.
- [14] Devaraj, S.J. (2019). Emerging paradigms in transform-based medical image compression for telemedicine environment. In *Telemedicine technologies*, 15-29.
- [15] Fatima, S. (2021). High speed data exchange algorithm in telemedicine with wavelet based on 4D medical image compression. *International Journal of Engineering and Management Research*, 11(4), 45-9.
- [16] Gowda, D., Sharma, A., Rajesh, L., Rahman, M., Yasmin, G., Sarma, P., Pazhani, A.A. (2022). A novel method of data compression using ROI for biomedical 2D images. *Measurement: Sensors*, 24, 100439.
- [17] Rani, M.L., Lavanya, V., SasibhushanaRao, G. (2021). Performance analysis of a hybrid method for medical image compression. *Turkish Journal of Computer and Mathematics Education (TURCOMAT)*, 12(14), 4478-85.
- [18] Vallathan, G., Jayanthi, K. (2021). An integrated and secured medical data framework for effective tele health applications. *International Journal of Advanced Intelligence Paradigms*, 18(1), 63-78.
- [19] Fred, A.L., Miriam, L.J., Kumar, S.N., Kumar, H.A., Padmanabhan, P., Gulyás, B. (2021). Lossless Medical Image Compression Using Hybrid Block-Based Algorithm for Telemedicine Application. In *Translational Bioinformatics Applications in Healthcare*, 147-171.
- [20] Monika, R., Dhanalakshmi, S. (2023). An efficient medical image compression technique for telemedicine systems. *Biomedical Signal Processing and Control*, 80, 104404.
- [21] Bindu, P.V., Afthab, J. (2021). Region of Interest Based Medical Image Compression Using DCT and Capsule Autoencoder for Telemedicine Applications. In 2021 Fourth International Conference on Electrical, Computer and Communication Technologies (ICECCT), 1-7.
- [22] Dhoub, D., Naït-Ali, A., Olivier, C., Naceur, M.S. (2021). ROI-based compression strategy of 3D MRI brain datasets for wireless communications. *IRBM*, 42(3), 146-53.
- [23] El-Shafai, Walid, E. Abd El-Samie, Fathi (2020), "Extensive COVID-19 X-Ray and CT Chest Images Dataset", Mendeley Data, V3.
- [24] Rojas-Hernández R, Díaz-de-León-Santiago JL, Barceló-Alonso G, Bautista-López J, Trujillo-Mora V, Salgado-Ramírez JC. (2022). Lossless medical image compression by using difference transform. *Entropy*, 24(7), 951
- [25] Gowda, D., Sharma, A., Rajesh, L., Rahman, M., Yasmin, G., Sarma, P., Pazhani, A.A. (2022). A novel method of data compression using ROI for biomedical 2D images. *Measurement: Sensors*, 24, 100439.
- [26] Rani, M.L., Lavanya, V., SasibhushanaRao, G. (2021). Performance analysis of a hybrid method for medical image compression. *Turkish Journal of Computer and Mathematics Education (TURCOMAT)*, 12(14), 4478-85.



© 2024 by Jins Sebastian, J. Deny and S.N. Kumar. Submitted for possible open access publication under the terms and conditions of the Creative Commons Attribution (CC BY) license (<http://creativecommons.org/licenses/by/4.0/>).